Fluid flow pattern and water residence time in waste stabilisation ponds

F. Badrot-Nico, V. Guinot and F. Brissaud

ABSTRACT

As treatment processes are kinetic-dependent, a consistent description of water residence times is essential to the prediction of waste stabilization ponds performance. A physically-based 3D transient CFD model simulating the water velocity, temperature and concentration fields as a function of all influent meteorological factors – wind speed and direction, solar radiation, air temperature and relative humidity – was used to identify the relationships between the meteorological conditions and the hydrodynamic patterns and water residence times distributions in a polishing pond. The required meteorological data were recorded on site and water temperatures recorded at 10 sampling sites for 141 days. Stratification events appear on very calm days for wind speeds lower than $3\,m\,s^{-1}$ and on sunny days for wind speeds lower than $5\,m\,s^{-1}$. De-stratification is related to two mixing processes: nightly convection cells and global mixing patterns. Numerical tracer experiments show that the results of the flow patterns can be evaluated using the dispersed flow regime approximation and, for wind speeds exceeding $6\,m\,s^{-1}$, the completely stirred tank reactor assumption.

Key words | fluid flow pattern, hydrodynamic model, temperature, waste stabilisation ponds, water residence times

F. Badrot-Nico
V. Guinot
F. Brissaud
Hydrosciences,
MSE,
Université Montpellier II,
Montpellier cedex 05,
Montpellier 34095,
France
E-mail: *fabiolabn@gmail.com*;
guinot@msem.univ-montp2.fr;
brissaud@msem.univ-montp2.fr

INTRODUCTION

As wastewater treatment depends on several kinetic processes, a consistent description of the hydrodynamic regime and particularly of the water Residence Time Distribution (RTD) is essential to the prediction of the removal of pollutants in Waste Sabilization Ponds (WSPs). Conceptual modelling of the hydrodynamic regime is widely used to predict the RTD and the performance of WSPs. Three different regimes may be considered: Completely Stirred Tank Reactor (CSTR), Dispersed Flow (DF) and Plug Flow (PF), the latter being too ideal to account for observed behaviours. Most authors (Marais 1974; Mayo 1995; Pearson *et al.* 1995; Brissaud *et al.* 2000) have used the CSTR model. According to Von Sperling (2002), the CSTR conceptual model is valid only for length to breadth ratios not significantly greater than unity. When the ratio of the length to the breadth exceeds unity, Von Sperling (1999, 2002, 2005) recommends considering a DF regime. The dispersion coefficient may be related to geometrical data such as pond length and breadth (Agunwamba *et al.* 1992). Thus, the pond geometry and the flow rate are the main factors that condition the RTD. While geometry may be the primary factor influencing pond hydrodynamic regime in tropical areas, additional factors, mainly meteorological, should be taken into account in other climates.

The actual RTD depends on the hydrodynamic regime generated by the local meteorological conditions. Unsteady meteorological conditions generate unsteady hydrodynamic regimes. Several types of hydrodynamic regimes may occur during one day. For instance, a frequently observed behaviour includes mixing under the influence of the wind, which may lead to a close-to-perfectly mixed regime, and periods of thermal stratification, over which the regime may be closer to dispersed flow. The RTD may be affected

doi: 10.2166/wst.2009.087

by the existence of short circuits and dead zones. Conceptual modelling is unable to represent the variations of hydrodynamic patterns due to meteorological conditions. Another approach such as three dimensional computational fluid dynamic (CFD) modelling is thus required to represent the hydrodynamic behaviour of WSPs, thus allowing for a better assessment of WSP performance.

Previous attempts in the field of three-dimensional CFD modelling of WSPs lacked an integration of boundary conditions taking into account the full influence of meteorological factors such as wind speed and direction, solar radiation, air temperature and relative humidity. In the work by Wood (1997), the wind influence was modelled by a fixed-velocity condition at the water surface. Thermal processes may strongly influence WSP hydrodynamic behaviour. Thermal modelling of WSPs was attempted by Salter (1999); however, solar radiation and air temperature were not included in the thermal model; the water surface and bottom temperatures were instead fixed to a constant value. Lately, Sweeney *et al.* (2005) modelled thermal stratification by computing the source terms due to the solar radiation, the advective heat, the free surface convection, the evaporative heat loss and the low temperature radiation. Wind speed was used to evaluate the thermal exchanges with the atmosphere, but not as a boundary condition for the hydrodynamics. Neglecting the wind effect on the hydrodynamics leads to a situation where only thermally-driven stratification breakdown can be modelled, whereas many authors report that WSPs hydrodynamics is mainly wind-driven (Frederik & Lloyd 1996; Salter 1999; Vorkas & Lloyd 2000).

The aim of this work is, through a combined use of field experiments data and a physically-based three-dimensional transient hydrodynamic CFD modelling, all relevant meteorological conditions and forcings being taken into account, to better understand the relationships between the meteorological conditions and the fluid flow pattern and RTD. The limits of CSTR and DF conceptual models will thus be pointed out.

MATERIALS AND METHODS

Temperature fields

Temperature measurements were undertaken in the last polishing pond of the Mèze (France) WSP, 43.36 °N, 3.53 °W (Picot *et al.* 2005). The pond area is about 1.7 ha and the depth is 0.90 m. Ten posts (Figure 1) were equipped with 5 temperature data loggers set at regular vertical intervals between the bottom and the water surface. The surface logger was allowed to float so that the water level fluctuations did not affect the recording of the surface temperature. The temperature sensors were HOBO® Water Temp Pro data loggers (ONSET Computer Corporation). Their resolution is 0.02°C and their accuracy ±0.2°C. Temperature measurements were carried out between early January 2005 and late June 2005. Infrared communication enabled on-site off-loading and continuous recordings. However, measurements were interrupted in February 2005, due to an ice-cover that had formed on the pond. Overall, the temperature fields were recorded for 141 days.

Meteorological data

An on-site weather station recorded at a five minute time step the air temperature and the relative humidity at a 3.5 m elevation, the solar radiation, the atmospheric pressure and the wind direction and average wind speed over five minutes at a 5.65 m elevation.

Mathematical model

The three-dimensional hydrodynamic model of the polishing pond was adapted from the COHERENS model (Luyten *et al.* 1990). The equations of Navier-Stokes and of the temperature are solved on a Cartesian grid to compute the three-dimensional (3D) currents and the temperature fields. The computational cells are 0.1125 m high and the horizontal

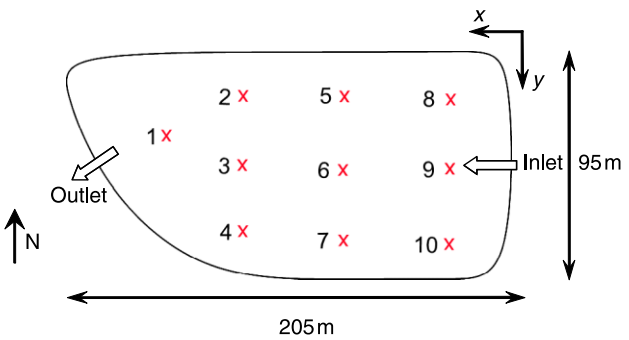

Figure 1 | Layout of the pond and location of the 10 temperature measurement sites.

grid dimensions extend from 1 m to 4 m, with a finer mesh close to the inlet, as recommended by Shilton (2001). The numerical scheme used for the resolution of the advection-diffusion equation is the Modified Discontinuous Profile Method (MDPM), a low-diffusion high-resolution scheme presented by Badrot-Nico *et al.* (2007). The boundary condition at the inlet is a fixed-velocity, fixed-temperature condition. Wind speed and direction, solar radiation, air temperature and relative humidity are introduced as forcings, through the definition of boundary conditions. The surface boundary conditions are assumed to be homogenous on the whole pond. Flow velocities, temperatures and concentrations are computed in each grid cell at each time step. The model was validated on temperature profiles and a tracer experiment (Badrot-Nico 2007).

RESULTS

Field observations

Thermal profiles

Observed temperature fields showed behaviours depending on the meteorological conditions. Thermal stratification events were defined as periods when the temperature gradient is larger than $0.6\,C.m^{-1}$, as given by Kellner & Pires (2002) and used by Sweeney *et al.* (2005). On the whole period, stratification events were found for 58 days, whereas no stratification occurred the other 83 days. Local stratification events duration ranged from 5 minutes to 19 hours and 35 minutes. Stratification was seen to appear during the day and never to persist over the whole following night. Temperatures at night were observed to become uniform on each vertical post and were horizontally homogenous over the whole pond with an accuracy of 0.2°C, even when the temperatures recorded during the day were not horizontally homogenous. The vertical temperature profiles were homogenous during a high percentage of time. From 65% of time in the May-June period to 81% in March and April, no stratification event was observed over the whole pond. Note however that deducing from a uniform temperature field that the pond is perfectly mixed would be misleading. Indeed, the main reason for the temperatures being observed (and later simulated) to be horizontally uniform is that the water surface boundary conditions, i.e. the air temperature, relative humidity and solar radiation, are uniform.

Temperatures measured at site 7 on 03/18/2005 and 03/31/2005 illustrate the influence of wind speed on stratification conditions. The main difference between these two days resides in wind speed values (Figure 2). The incident solar radiations were of the same order of magnitude; the air temperature was slightly higher on 03/31/2005, whereas the wind speed was about twice that of 03/18/2005. The measured air relative humidity was higher on 03/18/2005 than on 03/31/2005. On 03/18/2005 (Figure 3a), temperatures were homogenous in the pond during the night and at the end of the day, while thermal stratification occurred during the day. On 03/31/2005 (Figure 3b), no stratification build-up was observed and the thermal profiles at other sites were identical to those of site 7, which means that the pond was thermally horizontally homogeneous at all times of this day.

Statistical observations

The meteorological data and the temperature records were jointly analysed to identify the conditions of stratification build-up and destruction. This led to three types of meteorological conditions: favourable to stratification, unfavourable to stratification and undetermined. When the daily maximum wind speed was lower than $3\,m\,s^{-1}$, thermal stratification occurred even on cloudy days. The observed daily maximum solar radiation corresponding to thermal stratification with wind speeds lower than $3\,m\,s^{-1}$ ranged between $305\,W\,m^{-2}$ and $923\,W\,m^{-2}$. During sunny days, stratification events were observed each time the daily maximum wind speed was lower than $5\,m\,s^{-1}$; the observed daily maximum solar radiation ranged between $420\,W\,m^{-2}$ and $936\,W\,m^{-2}$ in these situations. Whatever the solar radiation was and up to a maximum observed daily solar radiation as high as $949\,W\,m^{-2}$, when the wind speed was higher than $6\,m\,s^{-1}$, no stratification was observed. More complex behaviours occurred when wind speed ranged between 3 and $6\,m\,s^{-1}$, especially for cloudy days when the solar radiation becomes temporarily very low.

The occurrence of stratification events at all sampling sites was studied during March to June 2005. In March and April 2005, stratification events occurred between 3.6%

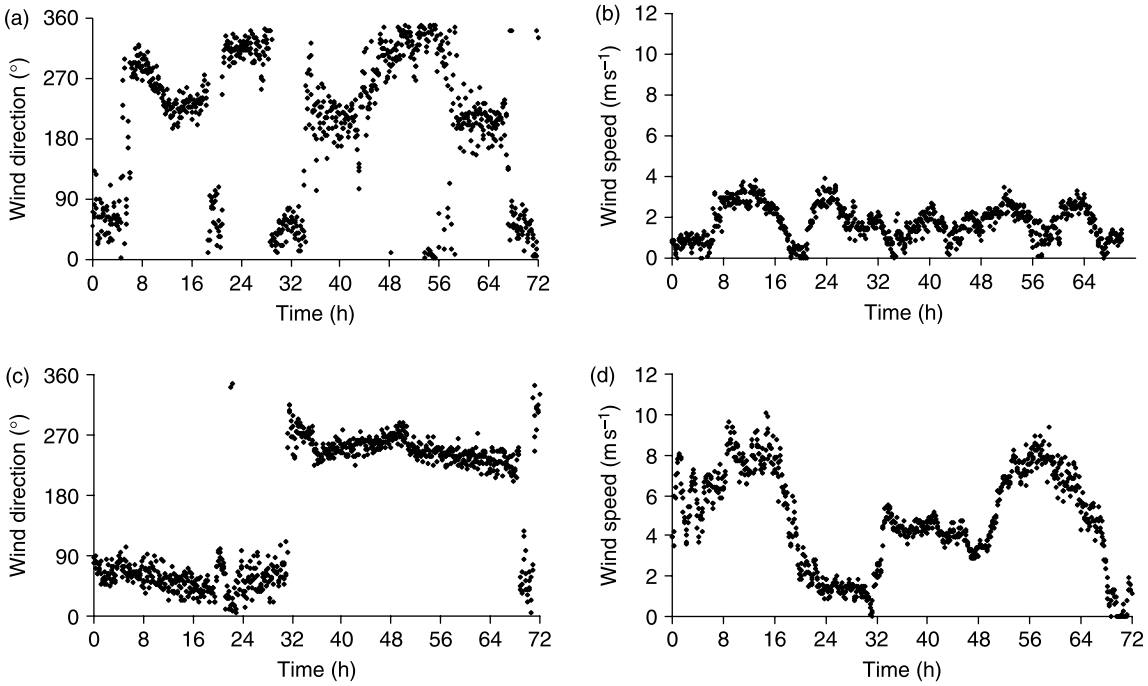

Figure 2 | Wind speed and direction recorded at the Mèze WWTP for 3 days from 03/18/2005 (a and b) and 03/31/2005 (c and d) at 00:00 am. Wind direction: N = 0 = 360, W = 90, S = 180, E = 270.

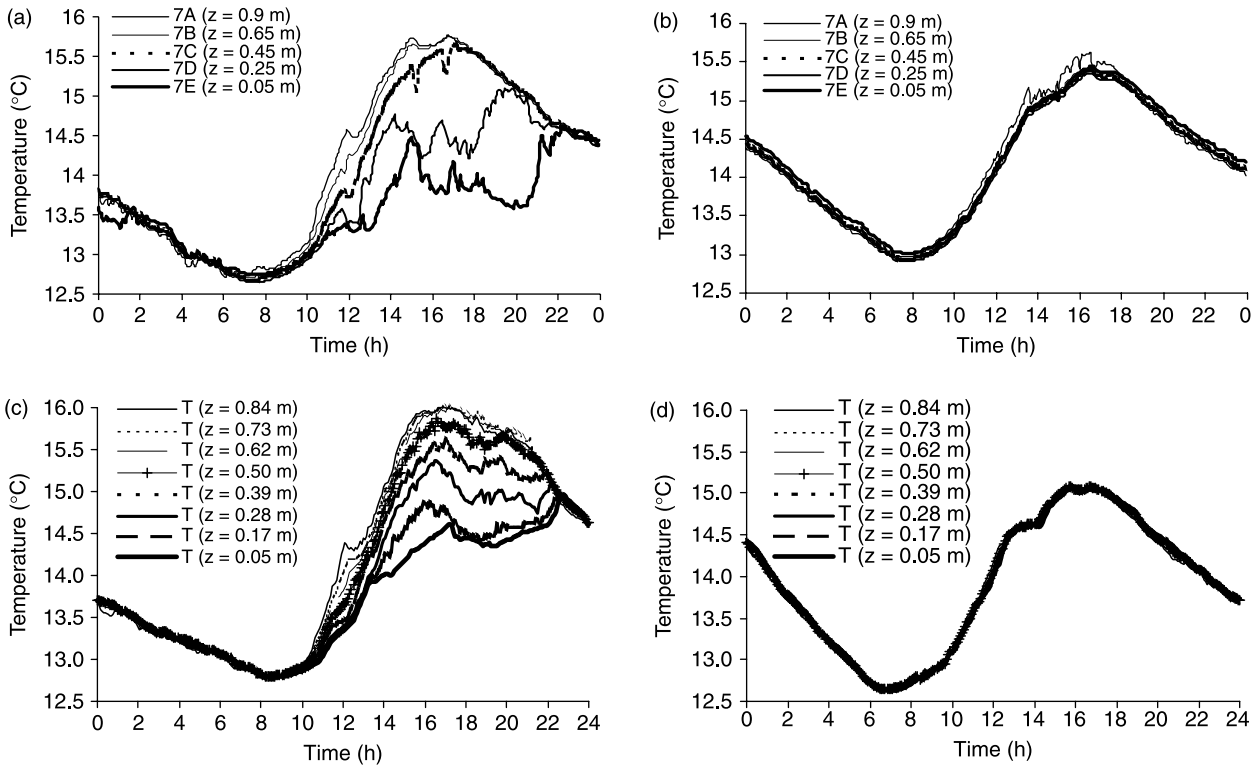

Figure 3 | Temperatures measured (a and b) and simulated (c and d) at site 7 with stratification (03/18/2005, a and c) and without stratification (03/31/2005, b and d).

(site 1) and 19% (site 3) of the time, and from late April to June between 2.8% (site 5) and 35% of the time (site 3). In both cases, the occurrence of stratification is higher on the North-West side of the pond (sites 1, 2, 5, 8), while stratification is less frequent on the South-East side and in the middle (sites 3, 4, 6, 7, 9, 10). In Mèze, the dominant winds blow from the North-West. The water surface being about 1.3 m lower than the top of the banks, these act as wind shields for the North-West part of the pond and the wind effect is stronger on the opposite side. Thus, stratification events occur mainly on the further upwind side with respect to the wind direction, which was also mentioned by Sweeney *et al.* (2005).

Numerical simulations

Simulated temperature profiles at site 7 on the 03/18/2005 and 03/31/2005 (Figure 3c and d) are compared to the experimental profiles of Figure 3a and b. The main features of the thermal profiles, i.e. night slope, starting stratification time, maximum gradient time etc., are well represented in both cases.

The plots of the currents within the pond at several times of the day show the prevalence of two main mixing structures: convection cells and wind-driven global mixing structures (Figure 4).

Convection cells

At night, wind speed is close to zero and vertical current structures appear, as shown in Figure 4a, for a very low wind speed (0.8 m s^{-1}). The surface temperature drops and this leads to a surface layer colder and denser than the water body: this unstable stratification generates vertical structures that are similar to convection cells. These convection cells result in the mixing of the water column and homogenous temperature vertical profiles. The size of the simulated vertical mixing cells is linked to the mesh dimensions; the real size of the convection cells could be determined by refining the mesh, but the computational time would be far higher. The validation of the CFD model showed that the size of the cells not being realistic does not burden with the accuracy of the computed temperature and solute concentration fields.

Global mixing structures

Simulated flow velocities in a slice of pond during daytime under a wind blowing from the North with a speed equal to

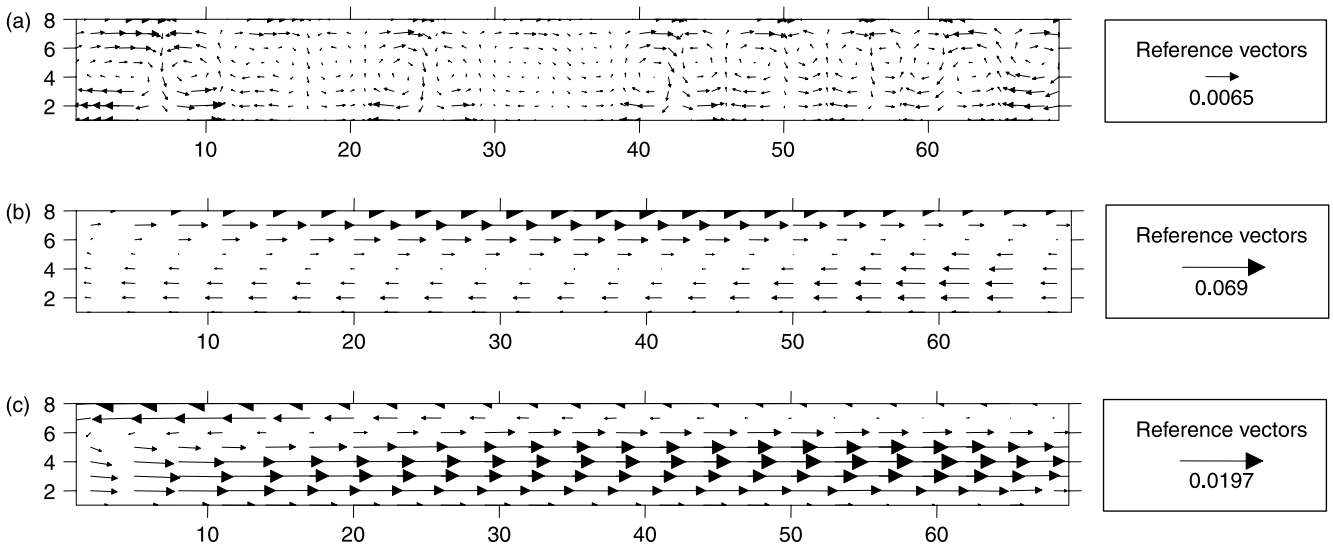

Figure 4 | Velocity field cross-sections at x = 190 m. Vertical mixing in convection cells on 03/17/2005 at 00:10 am, with a wind speed equal to 0.8 m s^{-1} (a). Strong wind conditions, with a wind speed of 8 m s^{-1} on 03/31/2005 at 10:00 am (b). Low influence of wind (2.5 m s^{-1}) on the 03/18/2005 at 3:00 pm (c). Space coordinates unit: m. Reference vectors unit: m s^{-1}.

8.5 m s^{-1} show a global circulation pattern with a reverse bottom current (Figure 4b). For this high wind speed value, the surface layer is dragged under the influence of the wind stress on the surface, and a reverse current appears at the bottom, as also shown by Fares & Lloyd (1995), Wood (1997) and Shilton (2001). For a lower wind speed (2.5 m s^{-1}), with a wind blowing from the West thus opposing the inlet-outlet direction, the influence of the wind stress appears to be less important (Figure 4c), with a thinner surface layer dragged in the wind direction; despite the existence of a global mixing structure a thermal stratification was observed and simulated. Thus, in some low wind cases, wind-induced currents are not strong enough to generate a complete mixing of the water column and body, and stratification can occur.

Residence time distributions (RTD)

Tracer tests were simulated starting on 03/18/2005 and 03/31/2005 (Table 1); on both days, the tracer was assumed being injected at 08:00 am, just before the potential stratification build-up, and in another run at 04:00 pm, when the potential stratification gradient was at its maximum. The wind speed and direction used as forcings during the 3 simulated days starting either from 03/18/2005 or 03/31/2005 are shown in Figure 2.

RTDs were obtained from the simulation of the tracer concentration at the pond outlet. The effect of wind is shown by the difference in RTDs under weak wind conditions (Figure 5a (run 1) and b (run 2)) and strong wind conditions (Figure 5c (run 3) and d (run 4)). Under

Table 1 | Bacteria removal calculated for the CSTR and DF regimes and the 4 numerical tracer experiments

	CSTR	DF	Run 1	Run 2	Run 3	Run 4
Injection time			03/18/2005 08:00 am	03/18/2005 04:00 pm	03/31/2005 08:00 am	03/31/2005 04:00 pm
Removal (log)	0.79	1.2	1.09	1.27	0.87	1.13

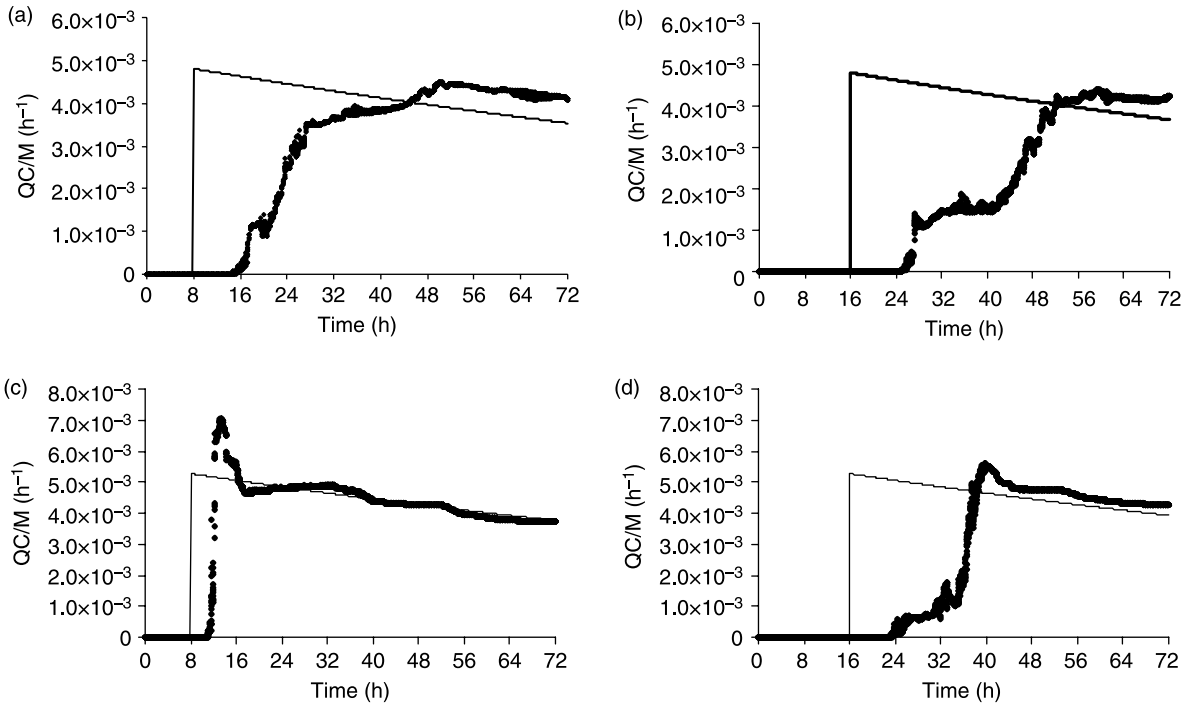

Figure 5 | Simulated RTD for runs 1 (a) to 4 (d). The CSTR curve (thin line) is plotted on each graph for comparison. Q = flow rate; C = tracer concentration; M = injected mass.

lasting strong wind conditions, complete mixing is quickly reached, but short circuiting may also occur (Figure 5c), while when the wind drops (Figure 5d) or has a low velocity (Figure 5a and b) the tracer reaches the outlet later and/or at lower concentrations. However, in every case, after less than two days, the tracer breakthrough curve behaves as would have resulted of a test in a CSTR. The influence of unsteady meteorological conditions is well illustrated by the effect of the tracer injection time on RTDs. When injected in a period of strong wind (run 3), preferential pathways appear and complete mixing is quickly reached; on the contrary, injecting the tracer 8 hours later when the wind starts dropping (run 4) result in a more progressive tracer recovery at the outlet of the pond. In every case, steep slopes of the RTD curve can be related to windy periods.

Modelling of bacteria removal

Bacteria removal can be estimated from RTDs on the 3 days following the tracer injection. These first days are indeed the most significant to calculate bacteria removal for most probable kinetic values (Brissaud *et al.* 2000). Bacterial decay was considered a first order kinetic reaction, with a die-off constant, $k_b = 0.6\,d^{-1}$, a value fairly representative of the influence of the weather conditions in March in Southern France. The dispersion coefficient, equal to 0.47, was computed from the formula by Von Sperling (1999), modified from Agunwamba *et al.* (1992), with $L = 205\,m$, $B = 95\,m$ and $H = 0.9\,m$. Bacteria removals derived from CFD modelling were compared to the removal calculated from the CSTR and DF models (Table 1).

All removals derived from the numerical tests are somewhat higher than those calculated from the CSTR model but close to the one obtained from the DF model. The removal derived from the numerical model is closer to the CSTR one on 03/31/2005, when the wind speed is high during the 8 hours following the injection set at 8 a.m.. A few percents only of the flow rate escape the perfect mixing pattern (Figure 5c). When the wind speed exceeds $6\,m\,s^{-1}$, the pond can be considered as totally mixed and CSTR an acceptable conceptual modelling choice despite the influence of some short-circuiting that affects bacteria removal. Lower wind speeds do not allow a complete mixing and bacteria removal for runs 1, 2 and 4 are about a factor 1.5 higher than with a CSTR model, mainly because short residence times are under-represented compared to a CSTR model (Figure 5a, b and d). Despite the mixing due to nightly convection structures, the transport of the tracer to the outlet is slower compared to wind-driven conditions. Such effects plead for the adoption of a DF model as recommended by Von Sperling (1999, 2002, 2005). As shown in Figure 4, even at speeds lower than $3.5\,m\,s^{-1}$, the influence of the wind stress on the water surface remains important and characterised by surface and bottom currents in opposite directions. Despite this behaviour and the effects of unsteady meteorological conditions, DF conceptual modelling appears to give an acceptable approximation of bacteria removal. This is somewhat surprising for DF conceptual model does not take the meteorological conditions into account.

For this order of magnitude of the die-off constant and except when the wind speed exceeds $6\,m\,s^{-1}$, the conceptual CSTR model allows for a pessimistic approximation of disinfection performance, while DF models are able to provide a satisfying approximation of the result of the pond hydrodynamic behaviour.

CONCLUSION

Monitoring the water temperature field over several months allowed identifying alternating stratification and de-stratification periods in the pond and relating these periods with the meteorological conditions. The predominant stratification process is the solar radiation heat gain, while sensible heat gain may also play a significant role when the solar radiation is low. De-stratification is due either to the wind effect or to the cooling of the upper water layers through the water surface by evaporative heat loss, sensible heat loss and mainly black body radiation at night.

The physically-based 3D transient CFD model enables elucidating the relationships between the meteorological conditions and the fluid flow patterns and RTDs. Stratification events appear on every very calm day with wind speeds lower than $3\,m\,s^{-1}$ and also on sunny days for wind speeds lower than $5\,m\,s^{-1}$. De-stratification processes are strongly linked to two mixing processes: the convection cells that

mainly occur at night, when the wind speed is low, and global mixing patterns that may appear when the wind speed is higher than about $2\,m\,s^{-1}$. Convection cells lead to a mixing of the water column and homogenous vertical temperature and solute concentration profiles. Wind speed higher than $6\,m\,s^{-1}$ forces a global mixing with a homogenous temperature field and nearly totally mixed although some short-circuiting may occur.

The numerical tracer experiments showed that the outcome of the fluid flow pattern of this pond can be fairly approximated as resulting of a CSTR for wind speeds exceeding $6\,m\,s^{-1}$ and, for lower wind velocities, of a DF hydrodynamic regime.

REFERENCES

Agunwamba, J. C., Egbuniwe, N. & Ademiluyi, J. O. 1992 Prediction of the dispersion number in waste stabilization ponds. *Water Res.* **26**(1), 85–89.

Badrot-Nico, F. 2007 *Modélisation tridimensionnelle des bassins de lagunage (3D modeling of waste stabilisation ponds)*. PhD Thesis, Montpellier 2 University, France.

Badrot-Nico, F., Brissaud, F. & Guinot, V. 2007 A finite volume upwind scheme for the solution of the linear advection-diffusion equation with sharp gradients in multiple dimensions. *Adv. Water Res.* **30**(9), 2002–2025.

Brissaud, F., Lazarova, V., Ducoup, C., Joseph, C., Levine, B. & Tournoud, M. G. 2000 Hydrodynamic behaviour and faecal coliform removal in a maturation pond. *Water Sci. Technol.* **42**(10–11), 119–126.

Fares, Y. & Lloyd, B. J. 1995 Wind effects on residence time in waste stabilization lagoons. *HYDRA2000*. Thomas Telford, London.

Frederik, G. L. & Lloyd, B. J. 1996 An evaluation of retention time and short-circuiting in waste stabilisation ponds using Serratia marcescens bacteriophage as a tracer. *Water Sci. Technol.* **33**(7), 49–56.

Kellner, E. & Pires, E. C. 2002 The influence of thermal stratification on the hydraulic behaviour of waste stabilization ponds. *Water Sci. Technol.* **45**(1), 41–48.

Luyten, P. J., Jones, J. E., Proctor, R., Tabor, A., Tett, P. & Wild-Allen, K. 1990 *COHERENS–A Coupled Hydrodynamical-Ecological Model for Regional and Shelf Seas*: User Documentation. MUMM Report, Management Unit of the Mathematical Models of the North Sea, pp. 914.

Marais, G. 1974 Faecal bacterial kinetics in waste stabilization ponds. *J. Environ. Eng. Division ASCE* **1**, 120–139.

Mayo, A. W. 1995 Modeling coliform mortality in waste stabilization ponds. *J. Environ. Eng.* **121**(2), 140–152.

Pearson, H. W., Mara, D. D. & Arridge, H. M. 1995 The influence of pond geometry and configuration on facultative and maturation waste stabilisation ponds performance and efficiency. *Water Sci. Technol.* **31**(2), 129–139.

Picot, B., Andrianarison, T., Gosselin, J. P. & Brissaud, F. 2005 Twenty years monitoring of Mèze stabilisation ponds. I–removal of organic matter and nutrients. *Water Sci. Technol.* **51**(12), 23–31.

Salter, H. 1999 *Enhancing the Pathogen Removal Performance of tertiary lagoons*. PhD Thesis, University of Surrey.

Shilton, A. 2001 *Studies into the hydraulics of waste stabilisation ponds*. PhD Thesis, Massey University, New Zealand.

Sweeney, D. G., Nixon, J. B., Cromar, N. J. & Fallowfield, H. J. 2005 Profiling and modelling of thermal changes in a large waste stabilisation pond. *Water Sci. Technol.* **51**(12), 163–172.

Von Sperling, M. 1999 Performance evaluation and mathematical modelling of coliform die-off in tropical and subtropical waste stabilization ponds. *Water Res.* **33**(6), 1435–1448.

Von Sperling, M. 2002 Relationship between first-order decay coefficients in ponds, CSTR and dispersed flow regimes. *Water Sci. Technol.* **45**(1), 17–24.

Von Sperling, M. 2005 Modelling of coliform removal in 186 facultative and maturation ponds around the world. *Water Res.* **39**, 5261–5273.

Vorkas, C. A. & Lloyd, B. J. 2000 The application of a diagnostic methodology for the evaluation of hydraulic design deficiencies affecting pathogen removal. *Water Sci. Technol.* **44**(10–11), 99–109.

Wood, M. G. 1997 *Development of Computational Fluid Dynamic Models for the Design of Waste Stabilization Ponds*. PhD Thesis, University of Queensland; Brisbane, Australia.